Original Paper

Landslides
DOI 10.1007/s10346-022-01892-w
Received: 26 November 2021
Accepted: 21 April 2022

F. A. Livio · A. Zerboni · M. F. Ferrario · G. S. Mariani · E. Martinelli · R. Amit

Triggering processes of deep-seated gravitational slope deformation (DSGSD) in an un-glaciated area of the Cavargna Valley (Central Southern Alps) during the Middle Holocene

Abstract Triggering mechanisms and causative processes of deep-seated gravitational slope deformations (DSGSD) in Alpine and high mountain areas include, among others, post-glacial debuttressing, earthquake-induced ground shaking, or co-seismic surface faulting. Distinguishing between climatic or tectonically driven factors is challenging since faults and fracture systems can play both an active and/or passive role in the process initiation. We applied an integrated approach, including morpho-structural analysis, geologic field survey, a paleoseismological approach applied to trenching, radiocarbon dating and detailed sedimentological analysis, to a DSGSD located in the Cavargna Valley (N Italy), an area that was never occupied by extensive ice tongues in the Upper Pleistocene and Holocene. We were able to document at least two phases of movement from the Middle Holocene onwards and related triggering factors. Thanks to the comparison with dated lacustrine turbidites in the Alpine Lakes, we argue a seismic triggering for the landslide onset, with a possible source located in southern Switzerland, close to the Insubric Line. The later evolution of the landslide was instead driven by climatic predisposing conditions (humid and cold), instead, corresponding to a phase of enhanced slope instability.

Keywords DSGSD · Prehistoric landslides · Seismic triggering · Climatic triggering

Introduction

Triggering mechanisms and/or causative processes of deep-seated gravitational slope deformations (DSGSD) in alpine and high mountain areas include, among others, post-glacial de-buttressing, earthquake-induced ground shaking, or co-seismic surface faulting, but they are generally hard to be identified. Distinguishing between climatic or tectonically driven factors can be particularly challenging since faults and fracture systems can play both an active and/or passive role in the process initiation, whereas the chronological correlation between DSGSD activation and climatic-driven increase instability requires precise radiometric dating. Nevertheless, this issue surely has significant implications for recent landscape evolution models as much as for paleoseismological studies and risk assessment.

A possible approach to face this issue is the dating of the onset and phases of activity of DSGSDs and a careful comparison with other external evidence of slope instabilities in the same region, looking for spatio-temporal clusters that would point to a triggering mechanism localized both in time and space (e.g., a seismic triggering). Conversely, a temporal cluster of evidence, more widespread over the entire region, possibly indicates a climatic driving factor, instead.

In this line, the surface expression of DSGSDs includes, especially in the uphill sector of the slope movement, morphostructural features such as double-crested ridges, counter slope curvilinear or straight scarps, open fissures, and morphological trenches (Onida 2001; Agliardi et al. 2001; Gutiérrez et al. 2009; Mariani and Zerboni 2020). These morpho-structures, generally characterized by ridge-top depressions bounded by fault scarps with opposite orientations, allow eluvial and/or colluvial sediments to be deposited, offering the opportunity to constrain the timing of onset and the evolution of gravity-driven slope deformations through a paleoseismological approach (Forcella et al. 2001; Tibaldi et al. 2004; Gutiérrez-Santolalla et al. 2005; Agliardi et al. 2009; Gutiérrez et al. 2009; McCalpin and Corominas 2019).

We applied an integrated approach to a DSGSD in a mountain area of northern Italy that was never occupied by extensive ice tongues in the Upper Pleistocene and Holocene and thus where slope unloading, due to the removal of glacial confinement, cannot be invoked. The case study is in the Cavargna Valley, N Italy (Fig. 1a), an area located outside the extent of the Alpine ice cap during Last Glacial Maximum (LGM) and only partially interested by small cirque glaciers. Thanks to an integrated approach, including morpho-structural analysis, geologic field survey, a paleoseismological approach applied to trenching, radiocarbon dating, and detailed sedimentological analysis, we were able to identify two phases of slope deformation and discuss between different causative mechanisms of both.

Geological, structural, and geomorphological setting

In the following paragraphs, we will outline the geological and geomorphological framework of the area, particularly focusing on its late Quaternary landscape evolution, to consider all the possible predisposing factors and causative processes of the DSGSD.

Regional setting

The study site is located in the European Southern Alps, close to the Tonale Line, a segment of the Periadriatic Lineament (Schmid et al. 1989) that accommodated through a dextral strike-slip motion the indentation of the Southern Alps against the Central Alps during the Oligo-Miocene.

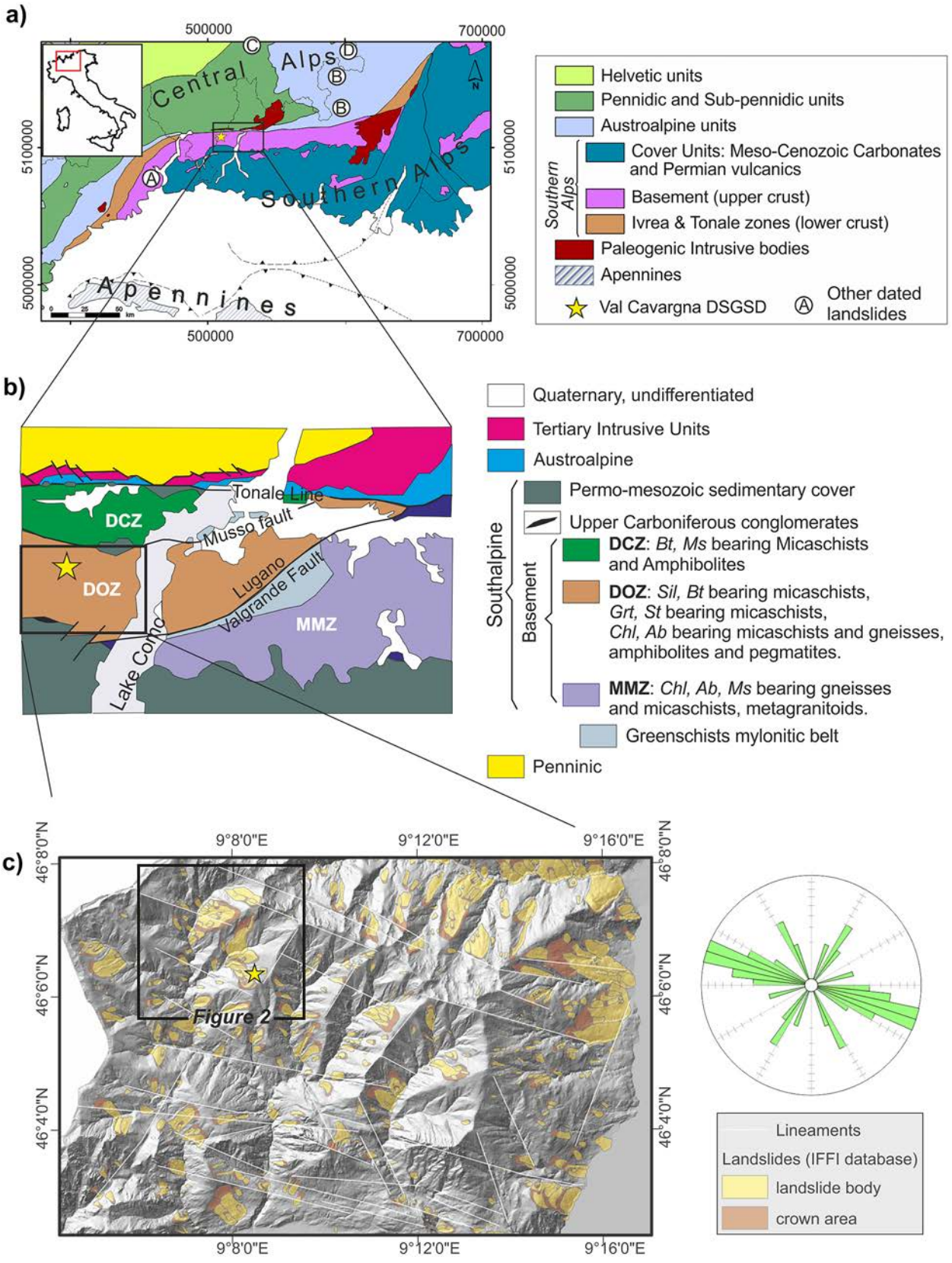
a)
500000
700000
5100000
5000000
Central Alps
Southern Alps
Apennines
A
B
C
D
Helvetic units
Pennidic and Sub-pennidic units
Austroalpine units
Southern Alps
Cover Units: Meso-Cenozoic Carbonates and Permian vulcanics
Basement (upper crust)
Ivrea & Tonale zones (lower crust)
Paleogenic Intrusive bodies
Apennines
Val Cavargna DSGSD
Other dated landslides
b)
Tonale Line
Musso fault
Lugano
Valgrande Fault
Lake Como
DCZ
DOZ
MMZ
Quaternary, undifferentiated
Tertiary Intrusive Units
Austroalpine
Southalpine
Permo-mesozoic sedimentary cover
Upper Carboniferous conglomerates
Basement
DCZ: Bt, Ms bearing Micaschists and Amphibolites
DOZ: Sil, Bt bearing micaschists, Grt, St bearing micaschists, Chl, Ab bearing micaschists and gneisses, amphibolites and pegmatites.
MMZ: Chl, Ab, Ms bearing gneisses and micaschists, metagranitoids.
Greenschists mylonitic belt
Penninic
c)
9°8'0"E
9°12'0"E
9°16'0"E
46°8'0"N
46°6'0"N
46°4'0"N
Figure 2
Lineaments
Landslides (IFFI database)
landslide body
crown area

◂**Fig. 1** **a** Regional geological sketch map of the Alps: the white circles indicate the locations of dated landslides nearby the study area (A, Tibaldi et al. (2004); B, Forcella et al. (2001); C, Poschinger et al. (2006); D, Agliardi et al. (2009); **b** Regional geological map with emphasis on the tectonic-metamorphic zones of the South Alpine basement in the Lake Como area: DCZ, Domaso-Cortafò Zone; DOZ, Dervio – Olgiasca Zone; MMZ, Mt. Muggio Zone (after, Spalla et al. 2002); **c** Shaded Digital Elevation Model (DTM 5 m; Regione Lombardia) with digitized lineaments (rose diagram on the right) and mapped landslides from the Italian landslide database (source: IFFI database, http://www.progettoiffi.isprambiente.it/cartanetiffi/progetto.asp?lang=EN); the yellow star indicates the study site in all the panels.

The region is characterized by extensive mass wasting and landslide phenomena (see, e.g., the Italian landslide inventory IFFI Project; https://www.isprambiente.gov.it/en/projects/soil-and-territory/iffi-project), including large DSGSDs (e.g., Pasquaré 2001; Ambrosi and Crosta 2006; Crosta et al. 2013; Agliardi et al. 2013), some of them provided with chronological constraints on their onset and evolutive steps (Forcella et al. 2001; Tibaldi et al. 2004; Poschinger et al. 2006; Agliardi et al. 2009).

Bedrock of the studied area belongs to a portion of the upper crustal tectono-metamorphic units of the Southern Alps (i.e., the Dervio – Olgiasca Zone – Fig. 1b; Spalla et al. 2002), located between two regional tectonic boundaries: the Musso Fault, to the N, and the Lugano – Valgrande Fault, to the south (Fig. 1). The Musso Fault is a cataclastic Alpine structure that was probably active at depth, during pre-Alpine tectonics (Siletto et al. 1990; Bertotti et al. 1993). The Lugano – Valgrande Fault is a Lower Jurassic normal fault that was later upturned during Alpine tectonics (Bertotti, 1991) and that is marked by the presence of a thick greenschist-facies mylonitic belt, where the deepest fault zone crops out (Fig. 1b).

In the study area, the Dervio-Olgiasca Zone, previously included by (Schumacher and Laubscher 1996) into the Val Colla – S. Marco Unit, consists of metapelites and metagranitoids. In particular, in the western sector of this tectono-metamorphic unit, the lithologies can be distinguished in: garnet-staurolite–bearing micaschists, chlorite-bearing micaschists, chlorite-albite–bearing gneisses, and metagranitoids, locally mylonitic (Fig. 1b; Spalla et al. 2002).

Brittle structures crosscutting through the bedrock, as emerging from a lineament analysis (Fig. 1c), show a predominant N110 direction, closely related to the local strike of the Lugano-Valgrande and Musso faults, with secondary modes at N30 and N150, possibly two Riedel systems of the former, formed during the dextral motion of the Tonale Line.

Study site

The study site is located at the head of Piazza valley (Fig. 2), a small ca. NE-SW trending tributary of the main Cavargna Valley. The Piazza valley is almost entirely interested by a DSGSD feature, ~ 1250 m wide and 1300 m long, which deformed the valley slope.

The valley presents a moderate relief energy, with an elevation drop of ~ 650 m (from 1750 to 1100 m asl) and is characterized by a steep down valley sector (~ 35–40°) and a gentler uphill slope (~ < 20°). An overall convex profile is marked by a clear break of slope between 1300 and 1400 m asl.

A considerable slope adjustment must be inferred for this region during the late Pleistocene, deeply interested by extensive glaciations and by periglacial and paraglacial processes. As common in the Alps, paraglacial environment, in particular, was influenced by post-glacial de-buttressing, fall of local base-level and gravitational adjustment of poorly vegetated slopes, following the retreat of glacial bodies (Knight and Harrison 2009). A detailed reconstruction of the recent geological and geomorphological evolution of the area is therefore a fundamental step for the understanding of the evolution and the causative processes of this DSGSD.

The Cavargna Valley DSGSD area and its surrounding were never interested by extensive glaciations in the Upper Pleistocene. According to Schlüchter et al. (2009), the main LGM ice cap reached an elevation of ~ 950 m asl; additionally, small cirque glaciers locally occupied the most elevated sectors of the Alps, typically above 1700 m asl, as highlighted by glacial and periglacial erosional landforms.

The area experienced a considerable regional deformation due to the isostatic answer to glacial retreat (post glacial rebound). Present-day uplift of the Alps is measured in ~ 1 mm/year through geodesy and remote sensing (e.g., Kahle et al. 1997; Gudmundsson 1994) and predicted that post-LGM rebound presumably contributes significantly to this value.

The temporal evolution of glacial withdrawal, bracketed through exposure dating of boulders and bedrock surfaces (Ivy-Ochs et al. 2006) highlights a very fast deglaciation phase along the southern Alps, starting from ~ 21 ka BP and leading to the almost complete dismantling of glaciers before 15 ka BP, thus implying a quick passage from full glacial conditions to a disequilibrium stage.

Finite–element modeling for the post-LGM isostatic rebound (Norton and Hampel 2010) highlights, for the site area, a displacement of ~ 90 m, cumulated between 21 and 13 ka BP and only ~ 10 m from 13 ka BP to present. The temporal evolution is thus characterized by a quick uplift in the first few thousands of years after glacial removal, followed by a long-lasting period of slow movement.

All the processes closely related to post-glacial rebound that could have caused and/or triggered slope mass movements (e.g., glacial seismotectonics and changes in local base-level) had therefore to be active in a time-window close to glacial withdrawal and, consequently, the onset and timing of DSGSD features, as well, have to be consistent and in time-dependency with these causative processes.

From this point of view, this case study is representative of the landscape morphology of high-altitude sectors in the whole Central Southern Alps, and can provide a significant contribution in analyzing slope instabilities non-related to paraglacial dynamics.

The area is covered by an extensive mapping of the active, inactive, and quiescent landslides (Fig. 1c; IFFI database – "Inventario dei Fenomeni Franosi in Italia" http://www.progettoiffi.isprambiente.it/cartanetiffi/progetto.asp?lang=EN; Trigila and Iadanza 2008; Trigila et al. 2010) that highlight the high density of instabilities in this high mountain catchment. More than 750 features were mapped in the IFFI database in Cavargna Valley: ~ 700 features are classified as rotational-translational or complex, 20 are rockfall-toppling and only 10 features are of flow type. This class distribution of the mapped

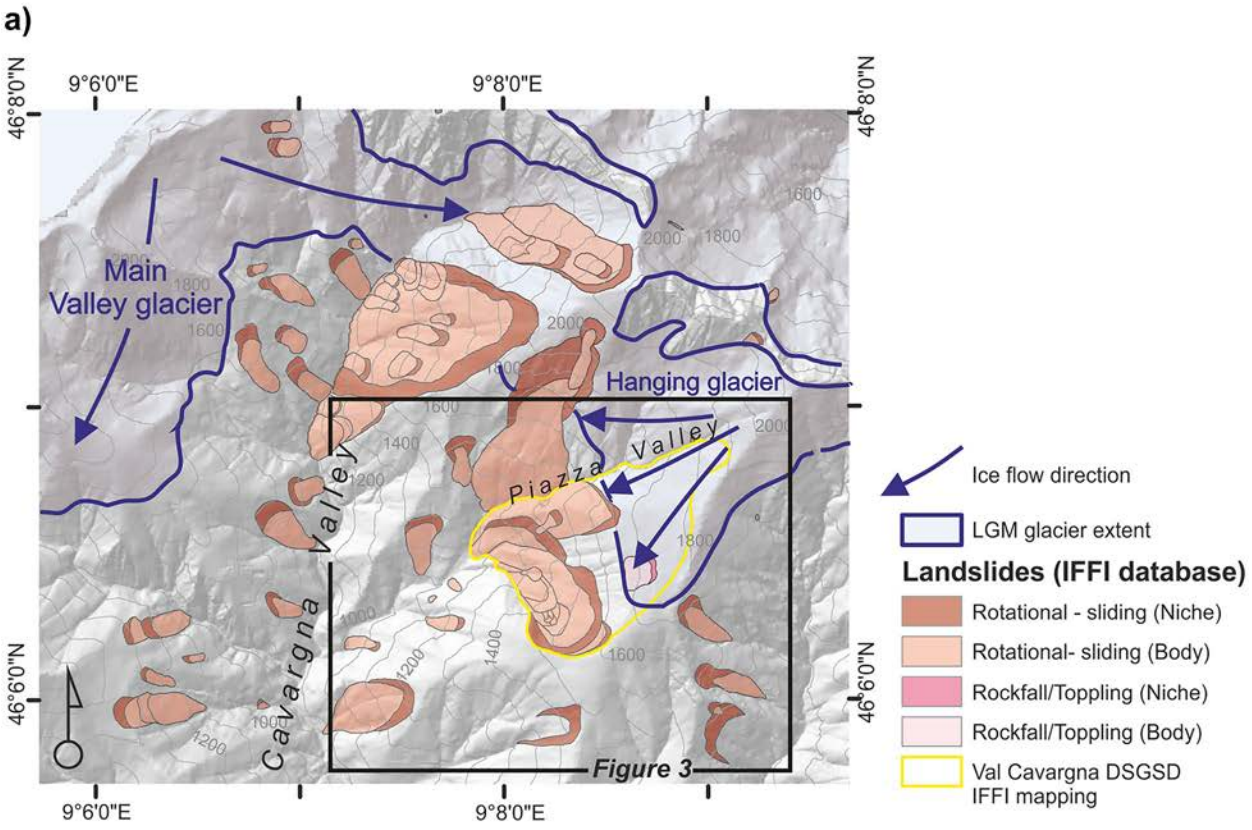
a)
9°6'0"E
9°8'0"E
46°8'0"N
46°6'0"N
Main
Valley glacier
Hanging glacier
Piazza Valley
Cavargna Valley
Figure 3
Ice flow direction
LGM glacier extent
Landslides (IFFI database)
Rotational - sliding (Niche)
Rotational- sliding (Body)
Rockfall/Toppling (Niche)
Rockfall/Toppling (Body)
Val Cavargna DSGSD
IFFI mapping

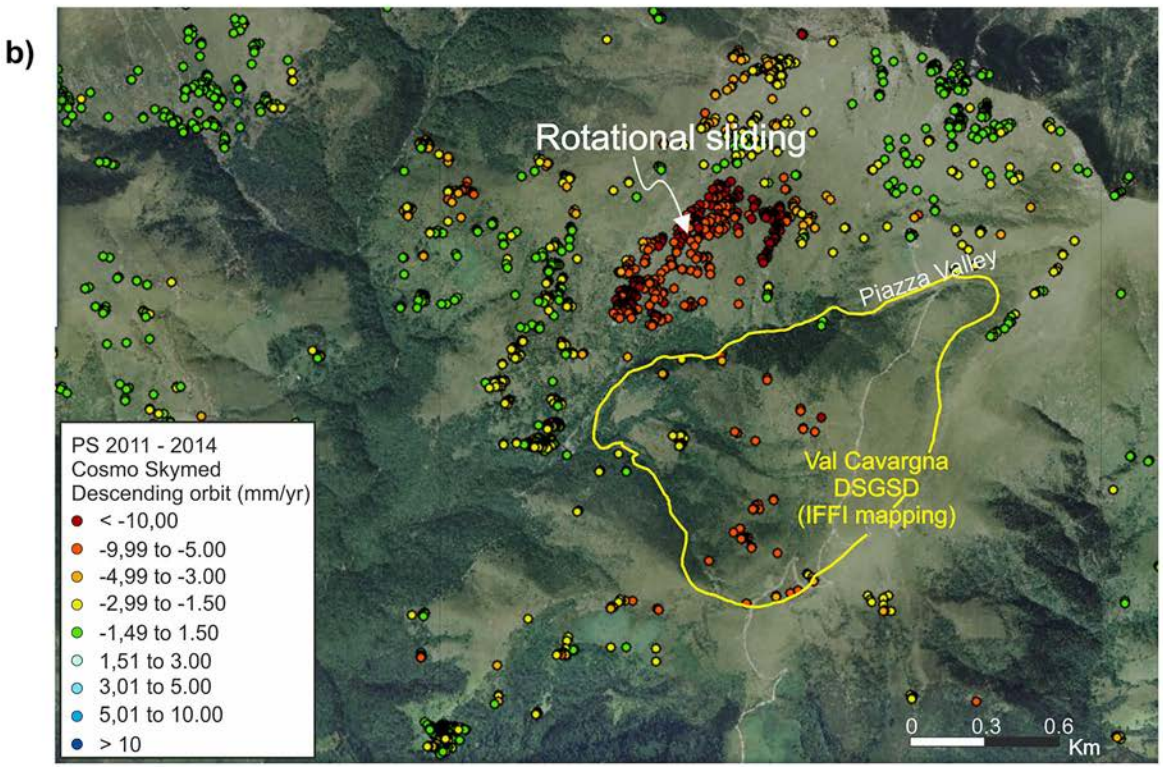
b)
Rotational sliding
Piazza Valley
Val Cavargna
DSGSD
(IFFI mapping)
PS 2011 - 2014
Cosmo Skymed
Descending orbit (mm/yr)
< -10,00
-9,99 to -5.00
-4,99 to -3.00
-2,99 to -1.50
-1,49 to 1.50
1,51 to 3.00
3,01 to 5.00
5,01 to 10.00
> 10
0 0.3 0.6
Km

◂**Fig. 2** **a** Digital elevation model of the valley showing the main landslides mapped according to the Italian national landslide catalogue (IFFI database–http://www.progettoiffi.isprambiente.it/cartanetiffi/). The maximum extent of the glaciers during LGM is also shown (Schlüchter et al. 2009); **b** Detail on the Cavargna Valley DSGSD with permanent scatterers velocities (along the line of sight; negative values for points moving away from the satellite) as detected by a Cosmo Skymed time series made available by the Italian Environmental Ministry and made available at http://wms.pcn.minambiente.it/ogc?map=/ms_ogc/WMS_v1.3/Vettoriali/Datafile_SAR_CSK_Descending.map

slope instabilities characterizes valley flanks that were subject to recent re-adjustment, with a limited thickness of shallow loose deposits and typically composed by basement lithologies.

Detailed geological field survey, conducted at 1:10.000 scale, and structural data collection allowed to recognize that the local structural setting played a role in predisposing the slope to deep seated deformations (Fig. 3).

The bedrock is widely outcropping along the slopes of the area, whereas landslide blocky deposits, later incised by the local drainage, are outcropping in the lower sectors of the valley. Rock foliation, here, considered also as a primary discontinuity driving possible slope movements, is moderately to highly dipping with an almost constant ca. N-S strike with most of the foliation planes dipping downslope, to the west. Meso-scale folding records a first deformation event (D1 in Fig. 3), ca. E-W directed, later involved into a NW–SE compressional event (D2 in Fig. 3), resulting in moderately expressed superposed folding structures. The area interested by the DSGSD is chaotically deformed, with pervasive jointing disrupting the rock mass.

Materials and methods

We performed a morpho-structural analysis by means of the photointerpretation of aerial stereo-photo pairs (acquisition year 1980, nominal scale 1:20.000) interpreted by means of an analogic SOKKIA stereo-viewer equipped with a 10 × magnifier.

Interpreted features have been later digitized in a GIS environment and compared with a 5 m spaced digital terrain model (Regione Lombardia, https://www.cartografia.servizirl.it/arcgis/services/wms/DTM5_RL_wms/MapServer/WMSServer). Geological and geomorphological field surveys were performed at 1:10.000 scale in a single survey season.

We excavated an exploratory trench in the niche area of the DSGSD to temporally constrain the onset and evolution of the DSGSD in the release zone by means of a traditional paleoseismological approach (e.g., McCalpin 2009). The trench is ~ 5 m long and 2.5 m deep.

The northern wall of the trench was cleaned and gridded with string, after which we drew a field trench log on graph paper at a scale of 1:20. Stratigraphic units were defined based on color, texture, and sedimentary structures and according to soil-forming processes. Soil horizons were identified according to the guidelines of the Food and Agriculture Organization (FAO 2006) and sampled for physical and chemical analyses, charcoal identification, and dating. The diagnostic soil horizons of buried palaeosols in the sequence were defined according to the international classification systems (Zerboni et al. 2011, 2015; WRB 2014; Soil Survey Staff 2014).

Particle size distribution was determined using laser diffraction (Malvern Mastersizer MS- 2000) after H_2O_2 and HCl treatments, according to the procedure described in (Crouvi et al. 2008), for removal of organic matter and precipitated carbonates, respectively.

The age of the polycyclic soil sequence was obtained by dating with radiocarbon (AMS-^{14}C) three samples of charcoal. AMS-^{14}C dating results were calibrated (2 s range) using the INTCAL20 curve (Reimer et al. 2020). The results of analyses and dating on soil horizons are reported in Zerboni et al. (2019); the reader is referred to that paper for the discussion of their significance in relation with the formation of the stratigraphic sequence.

Samples for charcoal analysis were wet washed through 4, 2, and 1 mm mesh sieves. The recovered fragments were analyzed using a Nikon Optiphot reflected light microscope at 50–400 × magnification (analyst: Gianalberto Losapio), on transverse, radial and tangential sections. Reference specimens of Laboratorio di Archeobiologia of Musei Civici of Como (Italy) as well as specialized literature (Schweingruber 1978, 1990) were used.

Results

Photointerpretation and morphostructural analysis

The SE flank of the Piazza Valley is occupied by an almost circular sector showing the typical characteristics of a deep-seated slope deformation (Figs. 4a and 5a). Following a detailed photointerpretation of the area, we re-mapped the extent of the DSGSD, slightly differing from the previously published IFFI one, being larger than previously thought (Fig. 4a).

An upper sector shows a gently dipping and regular profile, resulting from the erosive action of a hanging glacier (Fig. 2) and is crosscut by several ca. N-S trending lineaments and uphill-facing scarps, delimiting trench-like elongated depressions (Figs. 4a and 5b). This upper sector corresponds to the releasing niche area of the DSGSD, indicating an almost E–W directed extension. A major slope break separates this sector from the lower one (Fig. 4a), where secondary and shallower rotational slope deformations are expressed by typical arcuate niche scarps and slightly bulging at their feet. Bodies of terraced blocky landslide deposits, later incised by the drainage network, are present at the toe of the DSGSD (Fig. 5d). We can infer a relatively shallow lower shear plane for the DSGSD (~ 50–80 m below the ground level at maximum), as deduced from the envelope of the deformed sectors (Fig. 4b).

The extent of the deformed area is also confirmed by a structural analysis on the fracture distribution (Fig. 4a) with a drastic increase in the joint frequency observed at the survey stations located inside the interpreted DSGSD. Joint orientation is subparallel to the scarp strike in the upper sector or to the outer boundary of the landslide, whereas stations located outside the deformed area (e.g., VCA8, VCA11, and VCA13) record rare almost north-dipping joint systems.

Trenching

Trench stratigraphy and geochronology

We excavated an exploratory trench in the upper sector, across an elongated morphological depression (Fig. 5b). We exposed a

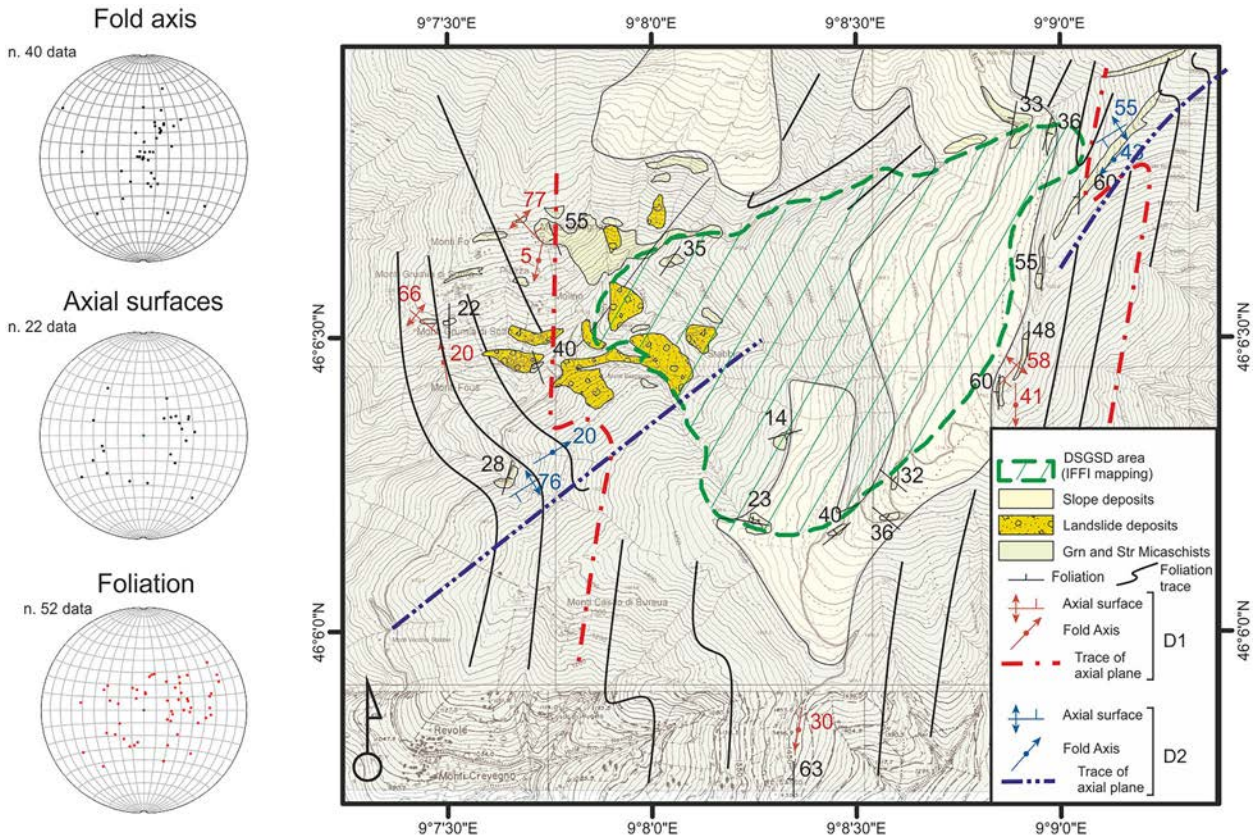

Fig. 3 Geological and structural sketch map of the study area: meso-structural data are reported in the stereoplots (Schmidt's lower hemisphere); D1 and D2 are deformational events, from older to younger

multiple sequence of slope/colluvial deposits weathered into soil horizons that cumulated in a depression bounded, at the sides, by two gravitationally driven normal faults (Fig. 6); subsequent colluvial events show a fining upward trend.

Sediments, deposited through colluvial slope processes, were subsequently weathered, and reorganized into a pedosequence of three stacked soils/paleosols (Fig. 6). For a detailed description of the (paleo) pedological setting of the trench, see a recent companion paper (Zerboni et al. 2019).

The uppermost unit 1 corresponds to the extant soil developed on a silty loam and differentiated into an upper organic A horizon and a lower Bw horizon. Below, unit 2 is a truncated and buried paleosol divided into three horizons: an eluvial 2E horizon occupies the upper position above a rubified 2Bs horizon. Intercalated in unit 2, there is a residual lens of macroscopic charcoal fragments, several centimeters thick, identified as the remains of an open-air hearth. Dating from two charcoal samples taken from the charcoal-rich lens gave a result of 2730 ± 43 and 2683 ± 42 years uncal BP (2932–2756 years cal BP and 2865–2743 years cal BP, respectively). The two samples are mainly composed of *Abies* charcoals, with presence of *Laburnum* cf. *alpinum*, *Picea/Larix*, and *Fagus* (Table 1). All the species are typical of high-altitude mountain settings, except for beech that is presently occupying areas at altitudes lower than 1400 m asl. Silver fir is the most common species, present at elevations up to 1800 m asl at least until the XVI cent. A.D. but presently almost lacking anywhere (Castelletti and Motella De Carlo 2012).

Below, at the bottom of unit 2, a 2BC horizon follows, with common reddish mottle. Unit 3 is an eluvial 3Et horizon on a silty clay, in which reddish mottles, comparable to those of the units above, are still present. Unit 4 is a weathered rubified 3Bs horizon that overlie a 3C (unit 5) horizon, the latter marking the boundary to the bedrock (unit 6) at about 150 cm below the present-day topographic surface. A charcoal fragment from unit 5 was dated to 6850 ± 20 years uncal BP (7733–7618 years cal BP).

The whole sequence is thickening up inside the fault-bounded depression (graben) and is crosscut by two conjugate sets of normal faults. The kinematic indicators are provided by the orientation of the clast's long axis, along a fault zone with characteristic shear fabric and indicating an almost pure dip slip kinematic, with less than 10% of horizontal component (Fig. 6). The bedding of the slope deposits is slightly dipping to the east, involved in a gentle synclinal folding with the beds getting steeper close to the fault (drag folding). Brittle secondary structures cut through units 4 and 3, displace the base of unit 2 as well, and die out upward inside unit 2 (i.e., fault concealment sensu Bonilla and Lienkaemper 1991). The movement of these faults is therefore postdating both the deposition of the parent material of unit 3 and its successive pedogenesis and the deposition of the lowermost unit 2.

Grain size distribution

The thickening of the units inside the graben reflects an increased sedimentation space that formed as the depression deepened and

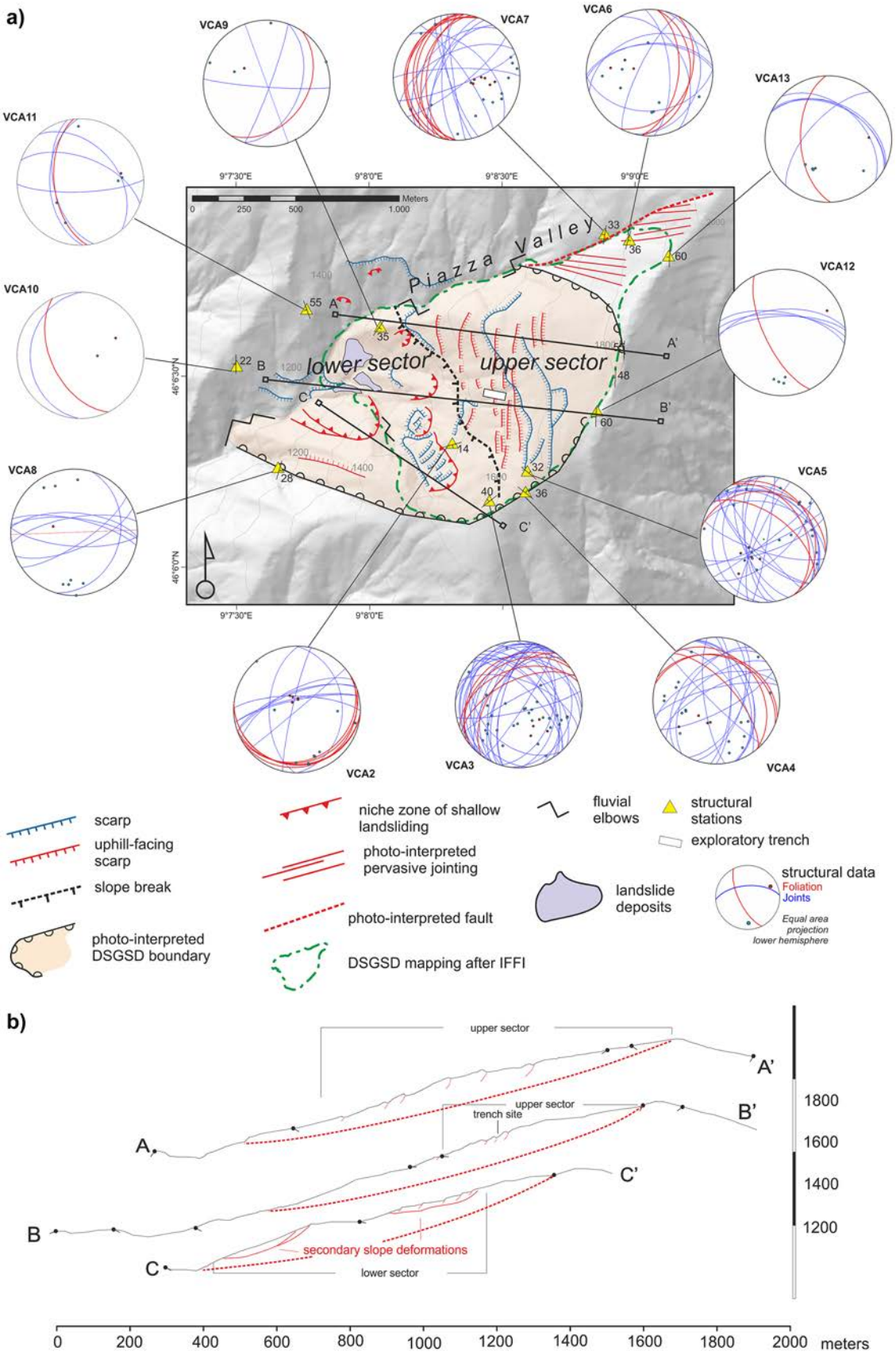

Fig. 4 **a** Photo-interpreted morpho-structural map of the Cavargna Valley DSGSD; measurement stations with structural data are also reported; **b** Topographic profiles with foliation orientations, main scarps and interpreted lower shear zone of the DSGSD.

Fig. 5 **a** Panoramic view on the Cavargna Valley DSGSD: location of the photos in the other panels are indicated; **b** View on one of the elongated depressions in the upper sector; **c** View of the exploratory trench, the bar is 1 m, location of the trench is indicated in panel b; **d** Terraced landslide blocky deposits located in the lower sector of the DSGSD.

widened through time. In order to unravel possible phases of increased movements and recognize events of surface rupture and reworking of slope deposits across the scarp, we proceeded with a high-resolution grain size analysis of the units.

We determined the particle grain size distribution of the uppermost four units. These were sampled (Fig. 6) both outside (H sample series) and inside the fault-bounded depression (G sample series).

Results are shown in Fig. 7: curves are presented coupled per sampled unit and after successive treatments for organic matter and $CaCO_3$ removal.

Overall, we note a good overlapping of the curves for the same units both in the H and G sampling locations, indicating a direct rework of the sediments from the hanging wall with no further weathering and a very limited transportation. Unit 1 is characterized by a predominant organic fraction, even in coarse aggregates (i.e., up to 50 mm). It shows an increase in the coarse inorganic fraction in the sample collected inside the trench (hundreds of mm), a fraction that is totally lacking in the H sample (located downslope) and that is thus indicating the occurrence of continuous colluvial events whose products were trapped in the depression.

Unit 2 shows a basal part (2 Gb) with a grain size curve perfectly overlapping with the H sample, indicating the same parent material, whereas the upper level (2 Ga) displays a marked shift toward the finer fraction, in all curves, possibly indicating a re-colluvium of sediments from the H sector into the depression, as also indicated by the erosive unconformity at the top of unit 2. Units 3 and 4, conversely, are almost perfectly matching in the H and G sectors.

Interpretation and discussion: characteristics and onset of the Cavargna Valley DSGSD

From the pedostratigraphy described above and considering the interpretation by Zerboni et al. (2019), the following evolution of the Cavargna Valley DSGSD can be inferred, basing on the restoration of the trench log (Fig. 8). Considering that the eastern end of the trench is not well exposed, we restored the trench basing on the cutoff, crosscut relationships, and folding against the western end of the depression.

At ~ 7.7 ka BP (step 0 in Fig. 8), unit 5 deposited as a coarse-grained slope/colluvial deposit. This happened in the early Middle Holocene (Davis et al. 2003), a period of climatic stability along the Southern Alps (Magny et al. 2009, 2012; Badino et al. 2018) that

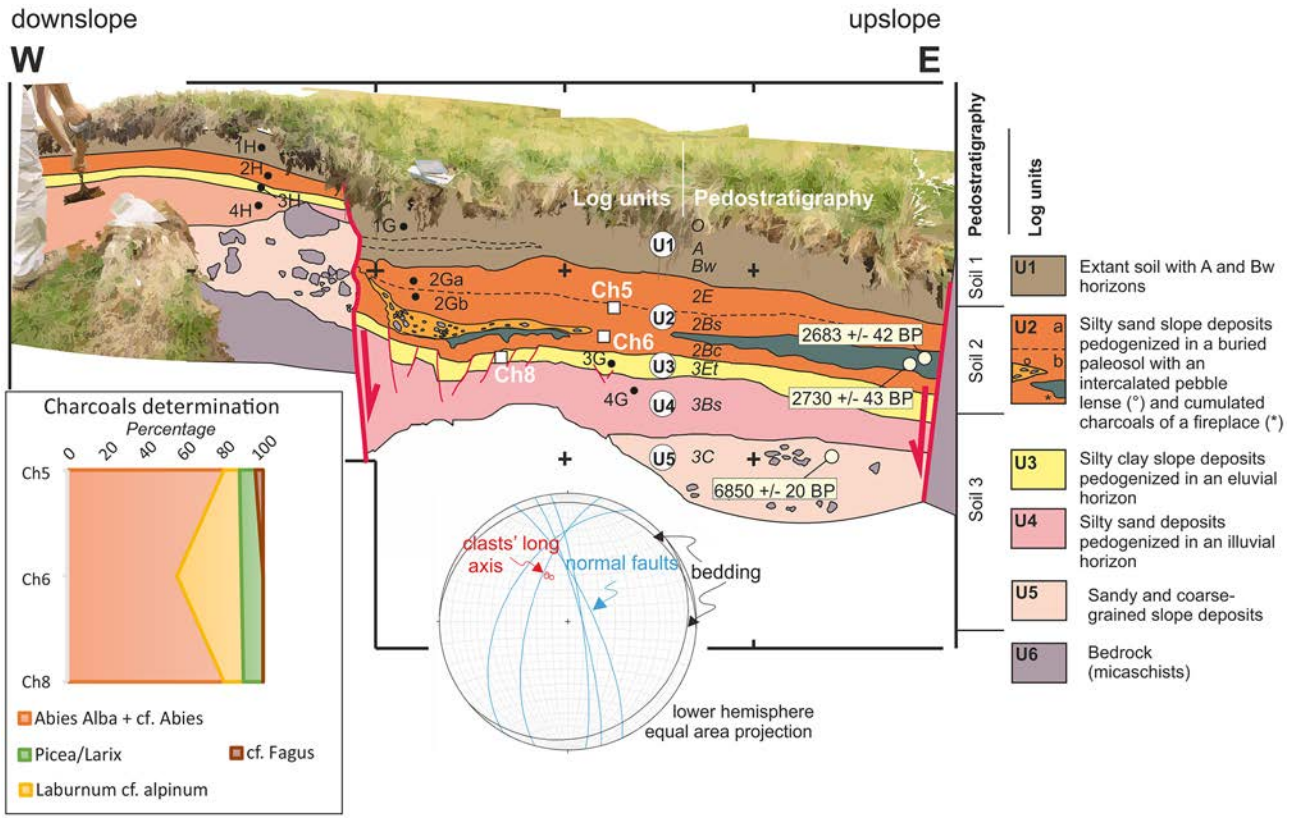

Fig. 6 Trench log (location in Figs. 4a and 5b) with the location of the samples for grain-size analysis (black dots), charcoal analysis (white square) and AMS-^{14}C dating (yellow dots); log units and pedostratigraphic horizons are also indicated

recorded, in Southern Europe, slightly colder average temperatures and increased precipitations in the whole Mediterranean area (Zanchetta et al. 2014).

We have no evidence of slope movements at that time or before. Conversely, the inception of the slope deformations happens at some time after, during the deposition of units 4 and 3 but before the development of soil 3 (step 1 in Fig. 8). We can consistently assume that the development of Soil 3 can be ascribed to a late Atlantic period, that ends up close to 5.0 ka BP (Mayewski et al. 2004; Zerboni et al. 2019). This offer a major constrain for the onset of slope failure and thus we can suggest that the landslide inception can be dated back between 7.7 and 5.0 ka BP; we record a displacement of 22 cm during this stage.

Then, deformation slowed down with only 24 cm of displacement cumulated up to step 2 (i.e., ~ 2.7 ka cal. BP; Fig. 8) and with a partial infilling of the fault-bounded depression due to the colluvial event in charge of the accumulation of unit 2.

Later deformation is due to a second pulse of slope movements (step 3) with several decimeters of offset displacing the buried soil 3 and the base of unit 2. Then, soil 2 developed, including an upper organic horizon that was later truncated by erosion.

Finally, a last phase of slow and continuous deformation, coupled with natural or human-driven colluvial activity and pedogenesis can be attested and probably dated back since the Roman warm period up to the present-day (Zerboni et al. 2019).

The evolution of the Cavargna Valley DSGSD records an almost continuous sequence of slope movements from the Middle Holocene onwards, far after the disintegration of the LGM ice cap. This fact and the fact that the area has never been interested by any major ice tongue let use to exclude that a major role in predisposing or triggering the mass movement has been played by glacial and post-glacial dynamics, including glacial debuttressing. We thus consider other processes including a climatic and/

Table 1 Charcoal taxa identification; for sample location see Fig. 6

Sample code and number of identified charcoals	Identified Taxa (%)			
	Abies Alba + cf. *Abies*	*Laburnum* cf. *alpinum*	*Picea/Larix*	cf. *Fagus*
Ch5 (n. 24)	80	8	8	4
Ch6 (n. 9)	56	33	11	-
Ch8 (n. 10 + 3 not determined)	80	10	10	-

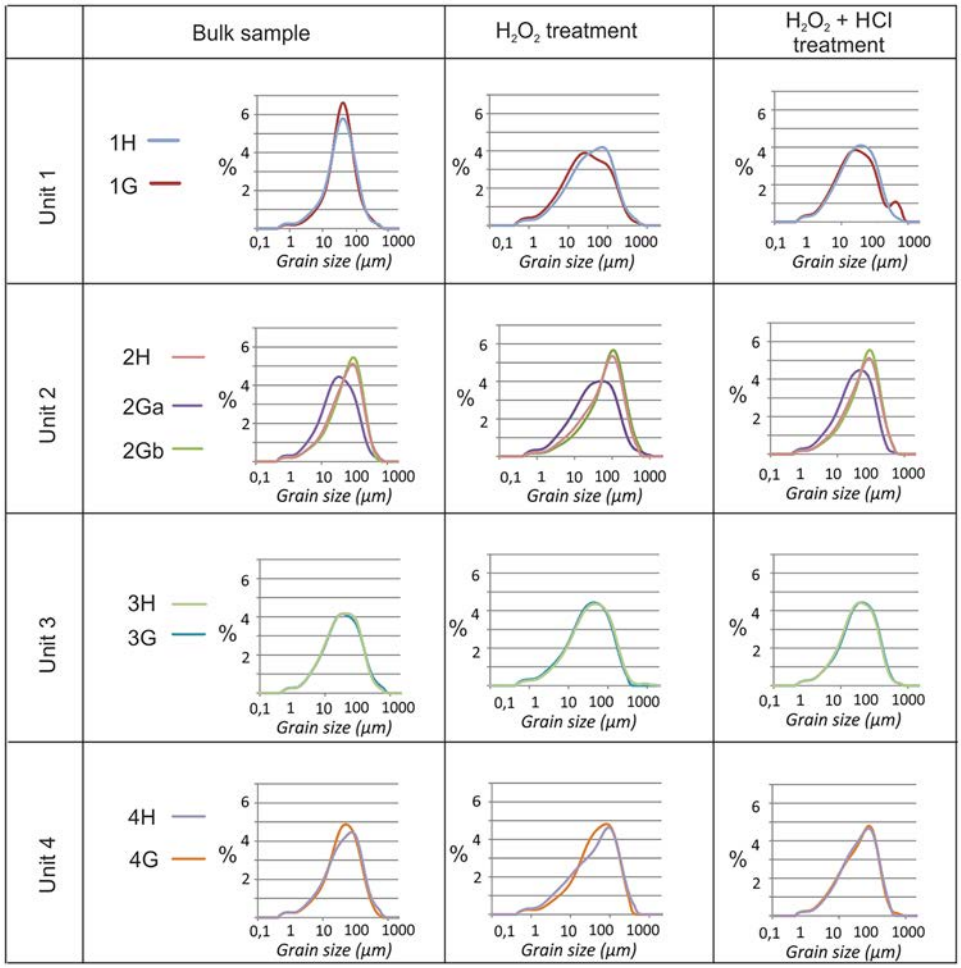

Fig. 7 Grain size distribution of the four uppermost units sampled both outside (H samples) and inside (G samples) the fault-bounded depression (sample location in Fig. 6); curves are presented after successive treatments of the bulk sample with H_2O_2 and HCl

or tectonic control on the landslide triggering; both of these two, possibly concurrent, triggering mechanisms have been invoked for known large landslides in the Alps, that seem to cluster in the same period (see e.g., Borgatti and Soldati 2010; Carbonel et al. 2013; Strasser et al. 2013; Zerathe et al. 2014; Oswald et al. 2021).

Seismic triggering is one of the major causes for large deep-seated landslides (e.g., Keefer 1984, 2000; Guzzetti et al. 2009; Delgado et al. 2011; Wang et al. 2019; Chunga et al. 2019). One of the possible supporting evidence for claiming a seismic triggering is the spatio-temporal clustering of large landslides, as observed also in the Alps (Sanchez et al. 2010; Zerathe et al. 2014) where a clustering of large events is ascribed to the subboreal chronozone (i.e., ~ 4.4–3.0 ka BP; Prager et al. 2008; Viganò et al. 2021; Oswald et al. 2021). Seismic shaking can also act as a weakening and predisposing factor for later landslides triggered by relatively moderate events, as also observed in offshore lacustrine records (Oswald et al. 2021). The onset of the Cavargna Valley landslide is ascribed to the Middle Holocene, a period when we record an apparently increased seismic activity in the whole Alpine chain (Schnellmann et al. 2002; Sanchez et al. 2010; Strasser et al. 2013; Kremer et al. 2017).

If we consider a seismic triggering for the pristine activation of this landslide, we must investigate the possibility that this could have been triggered by a seismogenic source included in the current seismotectonic setting of the chain. We thus consider a circular area, centered on the Cavargna Valley site and with radius of 250 km (Fig. 9) to identify all the possible sources triggering the earthquakes. This area corresponds to the maximum extent of the area affected by seismically-triggered landslides (Michetti et al. 2007), given an earthquake of maximum epicentral intensity X MCS (i.e., the upper bound for earthquakes in the Alpine seismotectonic setting; Dal Zilio et al. 2018). We proceeded with a simple buffer analysis, following the attenuation regressions for the maximum distance of seismically triggered landslides, given the earthquake epicentral intensity (Papadopoulos and Plessa 2000; Prestininzi and Romeo 2000). We conservatively considered an integrated upper bound relation, by adopting the maximum value from both the regressions for any given epicentral intensity. For any recorded earthquake from historical or instrumental catalogues (Fäh et al. 2011; Rovida et al. 2022), we buffered a region, around the epicenter, according to the regressions given above: none of the recorded strong earthquakes would have been potentially capable of triggering a landslide at the site (Fig. 9).

It results that either a presently unknown seismogenic source, closer to the site, must be supposed or a greater seismogenic potential must be invoked for some of the considered seismogenic sources. In the former hypothesis, there are several attested capable faults (ITHACA database; https://www.isprambiente.gov.it/en/projects/soil-and-territory/italy-hazards-from-capable-faulting-1?set_language=

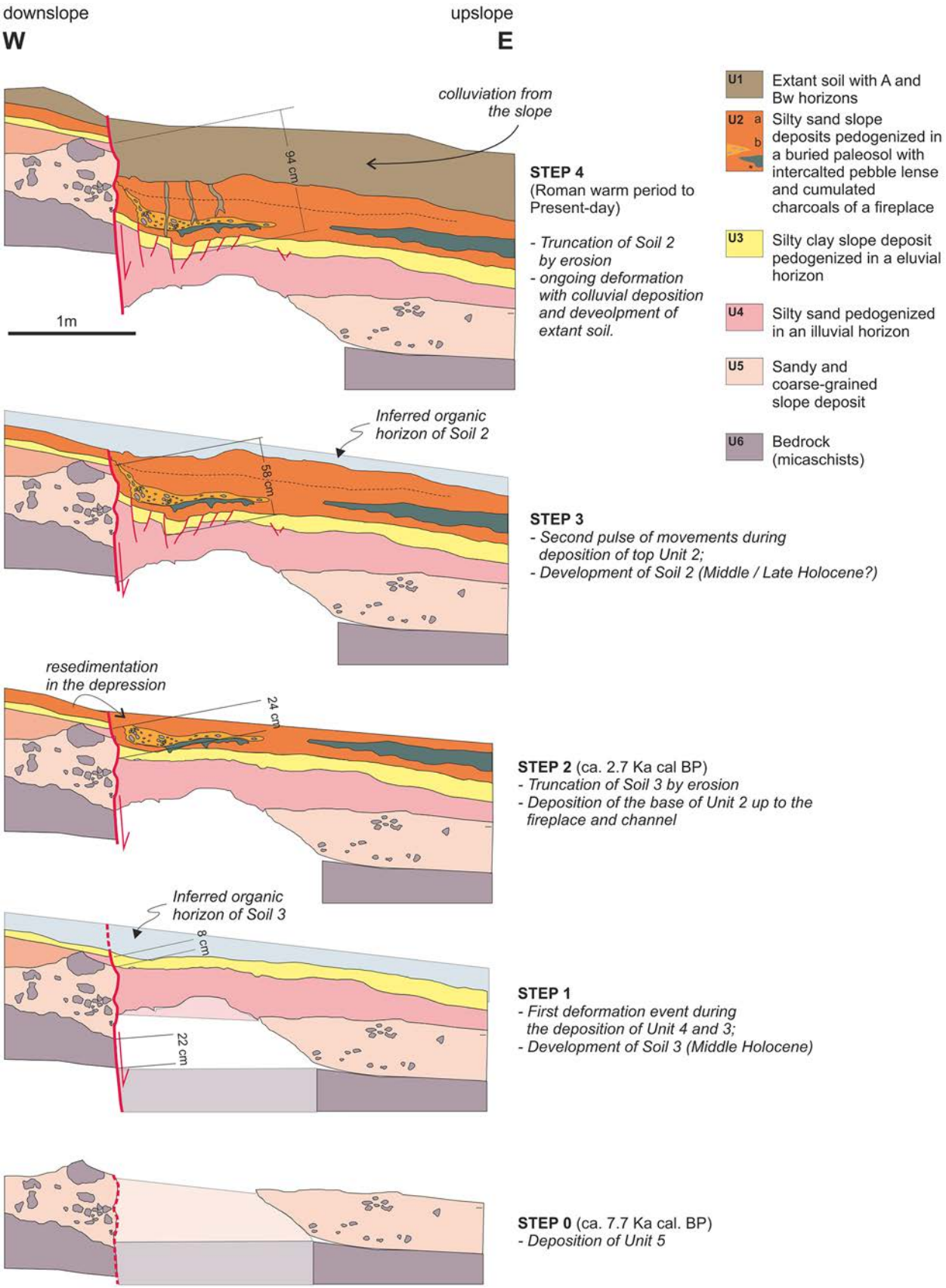

Fig. 8 Restoration of the exploratory trench from present day (step 4, top panel) to a pre-deformation geometry (step 0, bottom panel); cumulative offsets measured at the base of U3 are reported

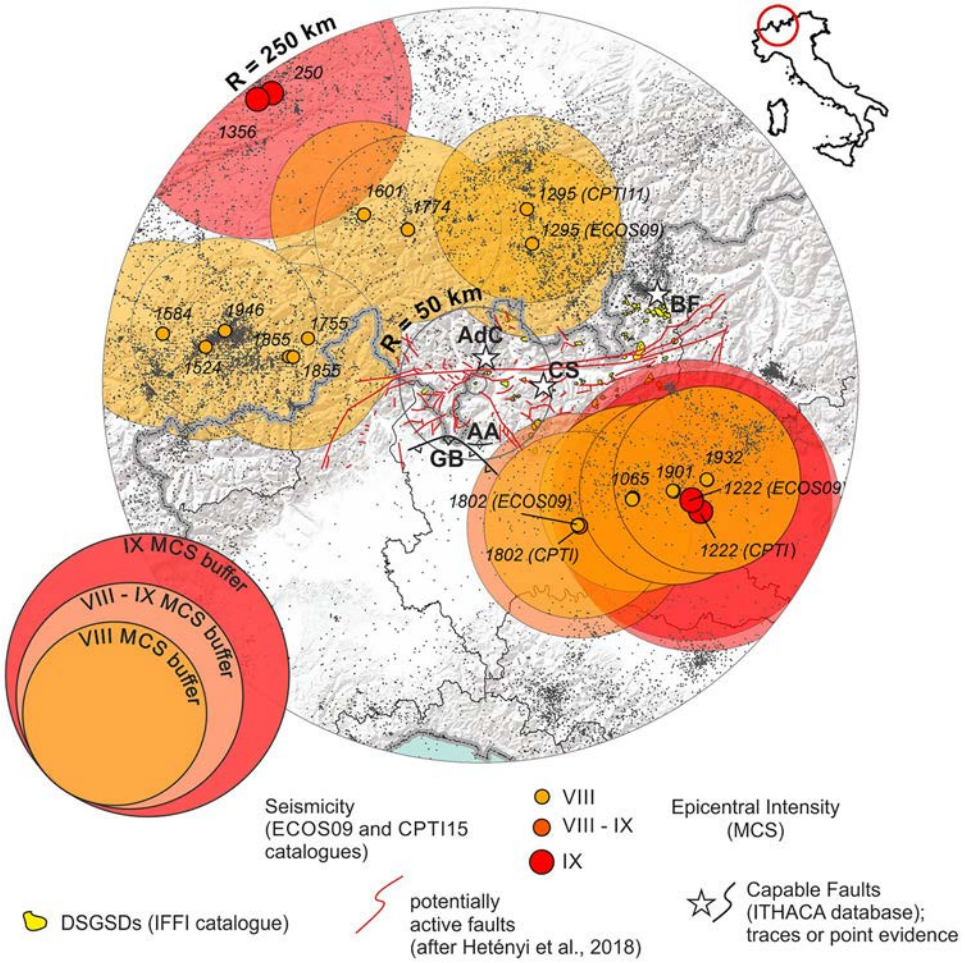

Fig. 9 Buffer analysis for a possible seismic triggering of the Cavargna Valley landslide, based on the analysis of instrumental and historical seismicity (Fäh et al. 2011; Rovida et al. 2022); capable (ITHACA database; https://www.isprambiente.gov.it/en/projects/soil-and-territory/italy-hazards-from-capable-faulting-1?set_language=en) and potentially active faults (Hetényi et al. 2018) are drawn in the closeness of the study site; see text for details. Codes: AA, Albese con Cassano Anticline; AdC, Alpe di Cauritt Fault; BF, Bormio Fault; CS, Cima Soliva Fault; GB, Gonfolite Backthrust

en) or potentially active faults (Hetényi et al. 2018) in the area not covered by the buffered region (Fig. 9). These include some structures located in the core of the Alps, such as the Alpe di Cauritt Fault, the Bormio Fault, and the Cima Soliva Fault (see locations in Fig. 9) and two major capable faults at the southern margin of the range: the Gonfolite Backthrust (Sileo et al. 2007) and the Albese con Cassano Anticline (Michetti et al. 2012).

In any case, external evidence such as a worldwide relationship between magnitude and plate convergence rates (Dal Zilio et al. 2018) and macroseismic data, as well (Locati et al. 2022), both indicate an upper magnitude bound of M_L 6.5 (i.e., I_o IX-X MCS) for the present day seismotectonic setting of the Central Alps.

Conversely, a possible hypothesis for claiming an increased seismotectonic potential in the Alps during past periods is related to a fast and transient crustal deformation induced by post-glacial rebound (Sanchez et al. 2010). Similar observations are widespread in the Fennoscandia shield area (Mörner 2004; van Loon et al. 2016) and in continental Europe (Brandes et al. 2015), where Late Glacial large earthquakes occurred with impressive frequency. A recent estimate of the post-glacial rebound in the Alps, based on an analytical solution for a half-space lithosphere of the Alps (Norton and Hampel 2010), predict ~ 100 m for the area close to the Cavargna Valley: 90 m regained during an initial fast phase of rebound (between 21 and 13 Ka BP) followed by a long-tailored slow deforming period when the remaining amount has been recovered. We expect that, if an increase of crustal deformation and, in turn, seismicity happened, this had to be synchronous with the crustal rebound or with a peak of frequency delayed only a few thousands of years, as observed elsewhere (Ballantyne et al. 2014a, b).

A climatic hypothesis must be considered as well; in fact, several authors suggest a Middle/Late Holocene climatic-triggered (re) activation of landslides and more in general slope instability in the southern Alps (Borgatti and Soldati 2010; Pelfini et al. 2014; Zerathe et al. 2014) and along the northern Apennine of Italy (Bertolini and Tellini 2001; Bertolini 2007). Even though the structural, seismic, and lithologic parameters oversee activation and dynamic of slope processes at different scales, it has been acknowledged that a higher frequency of rainfall and increased cooling led to (re)activation of landslides (Trauth et al. 2000, 2003; McGuire and Maslin 2012). In fact, increased rainfall and discharge and high fluctuations in precipitation, runoff and erosion cause significantly increased destabilization of slopes; moreover, the same factors influence the pore-water pressures lowering the critical thresholds in slopes susceptible to failure (Trauth et al. 2000; Guzzetti et al. 2007; Peruccacci et al. 2012; Segoni et al. 2018).

Records of flooding events are usually helpful in the reconstruction of rainfall fluctuations. Floods are related to the increased

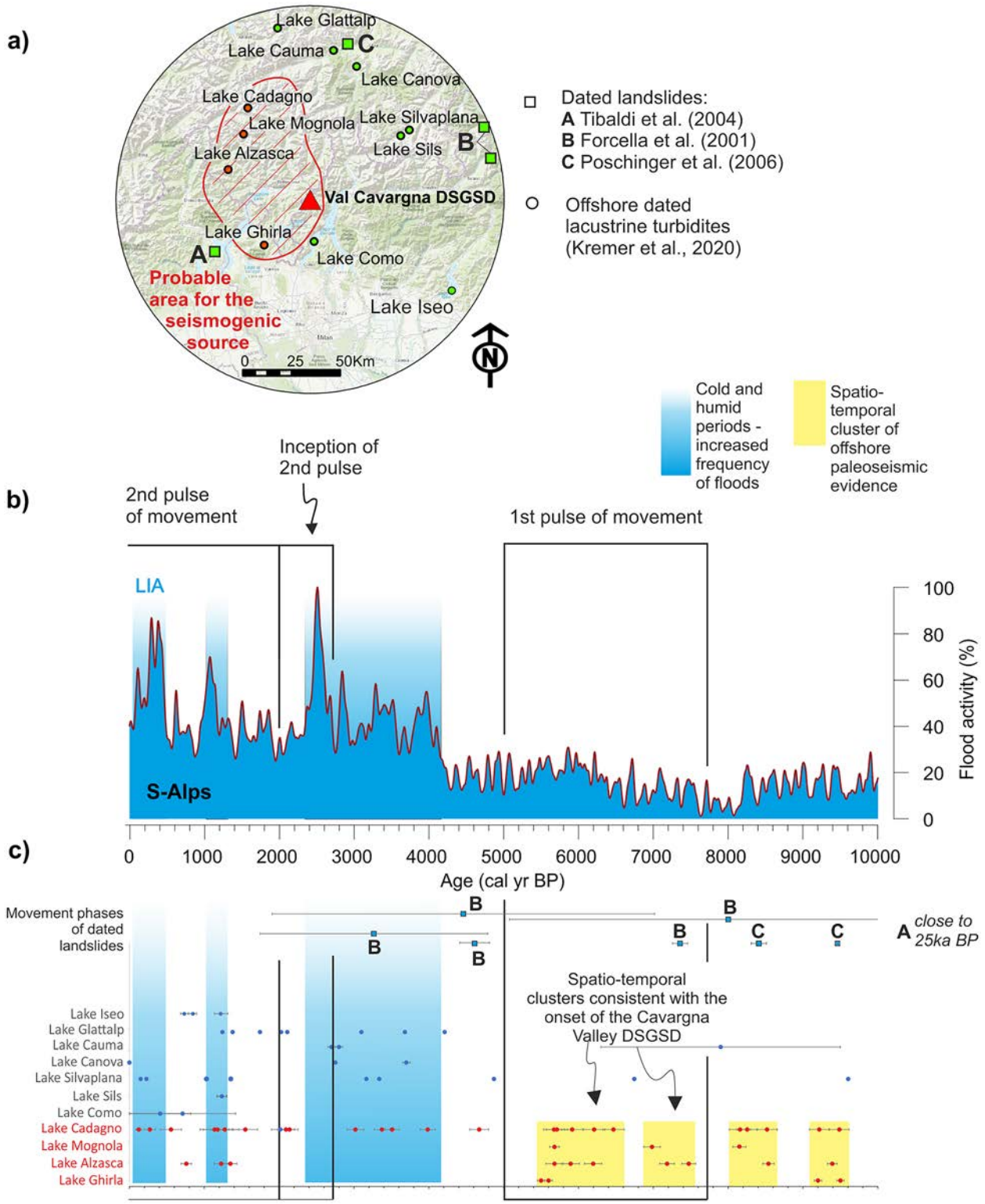

Fig. 10 Comparison of evidence for a climatic or seismic triggering for the Cavargna Valley DSGSD: **a** Location of offshore dated lacustrine turbidites (Kremer et al. 2020) and dated landslides (labeled as A, B, and C)within 100 km from the site: locations highlighted in red show a spatio-temporal clustering consistent with the Cavargna Valley site and potentially indicating a seismic triggering mechanism; **b** Stacked flood records for the Southern Alps spanning the past 10 kyr (Wirth et al. 2013) correlated with the timing of the Cavargna Valley landslide movements (blue-shaded areas indicate increased frequency of floods, including the latest period during the Little Ice Age–LIA); **c** Offshore evidence of paleoseismic events from dated lake turbidites in the Central Alps (Kremer et al. 2020; Rapuc et al. 2022 for Lake Iseo); see text for details

runoff caused by more precipitations. The same process also drives the start of rhexistasy phases and the development of slope instability. We used one of the longest offshore lacustrine records of flooding for the Southern Alps (Wirth et al. 2013); floods are related to increased runoff under rhexistasy phases (Erhart 1967), and the same setting generally promotes the activation of slope instability. According to this geological record, major flooding events are clustered at the 6.4–5.0 ka BP, 4.2–2.4 ka BP (with a peak at 2.6–2.4 ka BP) intervals, and during the Little Ice Age (Fig. 10). Other geomorphological and hydroclimatic records suggest, for the same intervals, glacial advances, cooler climatic conditions, fluctuating lake levels, and shifts in the timberline (see a review in Magny et al. 2009, 2012; Badino et al. 2018).

The seismic and climatic triggers are thus both reliable factors controlling the onset and evolution of the Val Cavargna DSGSD. In order to disentangle between the two hypotheses, we checked a possible spatio-temporal correlation between the onset of the pulses of landslide movements and hydroclimatic variability (Wirth et al. 2013) together with a dataset of offshore lacustrine paleoseismic indicators. Along the Alps, lacustrine turbidites have been identified in many cores and attributed to paleoseismicity (i.e., lacustrine turbidites; Kremer et al. 2020). Figure 10 illustrates the locations of offshore dated lacustrine turbidites and landslides inside a radius of 100 km around the study site.

The inception of the Cavargna Valley landslide, is poorly constrained in a quite long time window (i.e., 7.7–5.0 ka BP), but we noticed that it happened contemporary to a period which records two clusters of paleoseismic evidence (i.e., 7.3–7.0 ka BP and 6.5–5.5 ka BP), closely related in time and space (yellow intervals in Fig. 10b). Notably, other lakes, spreading farther to the NE, do not record a contemporary increase in the turbiditic events. The spatial distribution of the indicators, suggest that the likely location for the potential seismogenic source lies in the middle of the Ticino District (southern Switzerland) close to the Insubric Line; a seismic event at such location may have started the activity of the Cavargna Valley DSGSD. Yet, from the hydroclimatic point of view, the same time window lies across the switch from a warm period to one characterized by an increase in precipitations. We can suppose that the new climatic conditions could have contributed to promoting the movement of the Cavargna Valley DSGSD during the second part of this time window, but the spatial clustering of the evidence strongly suggest the triggering from a localized seismogenic source, instead.

The inception of the second pulse of movement (2.8–2.0 Ka BP) is closely temporally related to the peak in precipitations recorded by the lacustrine archives. Additionally, a widespread evidence of an increasing rate of turbiditic episodes is recorded in several lakes across the entire considered area (Fig. 10b), thus lacking a specific spatial clustering around the Cavargna Valley site. For the same period, a noteworthy contribution of human activities (wood clearance and herding) has possibly amplified the effect of the climate (Zerboni et al., 2019).

The role played by the climate conditions as a predisposing factor driving the evolution of such large landslides has to be carefully taken into account. Remarkably, the two phases of movement documented at the study site are coeval with cold and humid periods reconstructed in the Alpine region, in particular cold event CE3 between 7.5–6.9 ka BP and CE8 at 2.6–2.3 ka BP (Haas et al. 1998). The intensity of the first phase of cooling was relatively low and likely did not play a major role in the activation of the Val Cavargna DSGSD. On the contrary, several factors may have contributed to the reactivation of the DSGSD during the second phase, including lower temperatures, greater precipitations and all the environmental consequences of such processes: decrease in the local plant cover (negative shift of the treeline), increased periglacial conditions and formation of permafrost or even formation of small local glaciers. Such events have a clear effect on the reactivation of shallow slope processes (i.e., formation of colluvium), but their influence on deep movements is less evident.

In this perspective, we can thus propose that the onset of the Cavargna Valley landslide was triggered by seismic event(s), whereas its subsequent evolution is markedly influenced by climatic factors, thus highlighting a major shift in the factors overseeing the DSGSD dynamics.

We argue that, for settings similar to our case study, a combined action of enhanced seismicity and hydroclimatic conditions could be considered as both a triggering and predisposing factor: the progressive increase in the rock fatigue process and the reach of a critical state of the slope could in fact finally result in a major reactivation triggered by a moderate event (Gischig et al. 2016; Oswald et al. 2021).

Nonetheless, based on evidence, we suggest that the pristine activation of the landslide (initial Middle Holocene) occurred as a response to seismic activity, whereas subsequent pulses (late Holocene) of the structure seem to be much more correlated to phases of climatic instability. Likely, the structural weakness created by the initial event offered the proper conditions for subsequent climate-triggered reactivation of the landslide. Oscillations in climatic conditions and in the amount of precipitation are recorded throughout the Holocene at both millennial and centennial time scales (Magny et al. 2013).

Conclusions

In this study, we investigated a DSGSD in the Cavargna Valley (N Italy) through a morphostructural, pedostratigraphical, geomorphological, and paleoseismological approach. Dating and retrodeformation of the sedimentary sequence unearthed from an exploratory trench allow to document at least two phases of movement from the Middle Holocene onwards; the first pulse is bracketed at 7.7–5.0 ka BP, while the inception of the second pulse is dated at 2.8–2.0 ka BP.

We attempted to identify the triggering mechanism for the Cavargna Valley DSGSD by considering the historical earthquake catalog, a dataset of offshore lacustrine paleoseismological indicators and regional flood chronology. We exclude post-glacial debuttressing because the study region was never occupied by extensive glacial covers. Enhanced seismic activity related to postglacial rebound does not match the timing of the movements, so it can be excluded as well.

We conclude that a seismic triggering is likely for the onset of the DSGSD during the initial Middle Holocene, based on the spatio-temporal clustering with a set of offshore evidence, with a possible source located in an area lacking known historical seismicity or active faults, pointing to a possible knowledge gap in the seismotectonics of the Alps. Later evolution and successive pulses in the activity of the Cavargna Valley DSGSD (Late Holocene), instead, seem to be more correlated to regional proxies of climatic changes, showing a possible correspondence with periods of increased surface instability.

Understanding the timing and triggering mechanisms for DSGSD in Cavargna Valley and surrounding regions is paramount for reconstructing the local landscape evolution and eventually refine the implications for seismic hazard and for the cumulative effect of seismicity, structural weakness, and climatic instability.

Acknowledgements

The authors would like to thank Gianalberto Losapio for the identification and analysis of charcoal samples and Lanfredo Castelletti and Marco Tremari for the field reconnaissance that led to the site identification for trenching. Prof. Alessandro M. Michetti is also thanked the fruitful discussion and for the scientific coordination of the Interreg 2007-2013 "SITINET Project": during the field campaign under the umbrella of this project we firstly started the investigations here described.

Declarations

Competing Interests The authors declare no competing interests.

References

Agliardi F, Crosta G, Zanchi A (2001) Structural constraints on deep-seated slope deformation kinematics. Eng Geol 59:83–102. https://doi.org/10.1016/S0013-7952(00)00066-1

Agliardi F, Crosta GB, Frattini P, Malusà MG (2013) Giant non-catastrophic landslides and the long-term exhumation of the European Alps. Earth Planet Sci Lett 365:263–274. https://doi.org/10.1016/j.epsl.2013.01.030

Agliardi F, Crosta GB, Zanchi A, Ravazzi C (2009) Onset and timing of deep-seated gravitational slope deformations in the eastern Alps, Italy. Geomorphology 103:113–129. https://doi.org/10.1016/j.geomorph.2007.09.015

Ambrosi C, Crosta GB (2006) Large sackung along major tectonic features in the Central Italian Alps. Eng Geol 83:183–200. https://doi.org/10.1016/j.enggeo.2005.06.031

Badino F, Ravazzi C, Vallè F et al (2018) 8800 years of high-altitude vegetation and climate history at the Rutor Glacier forefield, Italian Alps. Evidence of middle Holocene timberline rise and glacier contraction. Quatern Sci Rev 185:41–68. https://doi.org/10.1016/j.quascirev.2018.01.022

Ballantyne CK, Sandeman GF, Stone JO, Wilson P (2014a) Rock-slope failure following Late Pleistocene deglaciation on tectonically stable mountainous terrain. Quatern Sci Rev 86:144–157. https://doi.org/10.1016/j.quascirev.2013.12.021

Ballantyne CK, Wilson P, Gheorghiu D, Rodés À (2014b) Enhanced rock-slope failure following ice-sheet deglaciation: timing and causes. Earth Surf Proc Land 39:900–913. https://doi.org/10.1002/esp.3495

Bertolini G (2007) Radiocarbon dating on landslides in the NorthernApennines (Italy), in: Landslide and Climate Changes: challenges and solutions, edited by: McInnes, R., Jakeways, J., Fairbank, H., and Mathie, E., Taylor & Francis Group, London, 2007

Bertolini G, Tellini C (2001) New radiocarbon dating for landslide occurrence in the Emilia Apennines (Northern Italy)Fifth Int. Conf. on Geomorphology, Tokyo, 23rd–28th August 2001. Abstracts of conference papers, Transactions JGU, vol. 22(4) (2001)

Bertotti G (1991) Early Mesozoic extension and Alpine shorteningin the western Southern Alps: the geology of the area betweenLugano and Menaggio (Lombardy, Northern Italy). Mem Sci Geol 43:17–123

Bertotti G, Siletto GB, Spalla MI (1993) Deformation and metamorphism associated with crustal rifting: The Permian to Liassic evolution of the Lake Lugano-Lake Como area (Southern Alps). Tectonophysics 226:271–284. https://doi.org/10.1016/0040-1951(93)90122-Z

Bonilla MG, Lienkaemper JJ (1991) Factors affecting the recognition of faults exposed in exploratory trenches. Bulletin. Geological Survey, Alexandria, VA (United States)

Borgatti L, Soldati M (2010) Landslides as a geomorphological proxy for climate change: a record from the Dolomites (northern Italy). Geomorphology 120:56–64

Brandes C, Steffen H, Steffen R, Wu P (2015) Intraplate seismicity in northern Central Europe is induced by the last glaciation. Geology 43:611–614. https://doi.org/10.1130/G36710.1

Carbonel D, Gutiérrez F, Linares R et al (2013) Differentiating between gravitational and tectonic faults by means of geomorphological mapping, trenching and geophysical surveys. The case of the Zenzano Fault (Iberian Chain, N Spain). Geomorphology 189:93–108

Castelletti L, Motella De Carlo S (2012) Il fuoco e la montagna. Archeologia del Paesaggio dal Neolitico all'Età Moderna in alta Val Cavargna. Castelletti, Lanfredo; Motella De Carlo, Sila, Como

Chunga K, Livio FA, Martillo C et al (2019) Landslides triggered by the 2016 Mw 7.8 Pedernales, Ecuador Earthquake: correlations with ESI-07 intensity, lithology, slope and PGA-h. Geosciences 9:371. https://doi.org/10.3390/geosciences9090371

Crosta GB, Frattini P, Agliardi F (2013) Deep seated gravitational slope deformations in the European Alps. Tectonophysics 605:13–33

Crouvi O, Amit R, Enzel Y et al (2008) Sand dunes as a major proximal dust source for late Pleistocene loess in the Negev Desert, Israel. Quatern Res 70:275–282. https://doi.org/10.1016/j.yqres.2008.04.011

Dal Zilio L, van Dinther Y, Gerya TV, Pranger CC (2018) Seismic behaviour of mountain belts controlled by plate convergence rate. Earth Planet Sci Lett 482:81–92. https://doi.org/10.1016/j.epsl.2017.10.053

Davis BAS, Brewer S, Stevenson AC, Guiot J (2003) The temperature of Europe during the Holocene reconstructed from pollen data. Quatern Sci Rev 22:1701–1716. https://doi.org/10.1016/S0277-3791(03)00173-2

Delgado J, Peláez JA, Tomás R et al (2011) Seismically-induced landslides in the Betic Cordillera (S Spain). Soil Dyn Earthq Eng 31:1203–1211. https://doi.org/10.1016/j.soildyn.2011.04.008

Erhart H (1967) La génèse des sols en tant que phénomène géologique. Masson édit., Paris, 83 pp

Fäh D, Giardini D, Kästli P et al (2011) ECOS-09 earthquake catalogue of Switzerland release 2011 report and database. Public catalogue, 17. 4. 2011. Swiss Seismological Service ETH Zurich. RISK

FAO (2006) Guidelines for soil description. Food and Agriculture Organization of the United Nations, Rome

Forcella F, Tibaldi A, Onida M, Galadini F (2001) Tecniche paleosismologiche per lo studio di deformazioni gravitative profonde di versante in ambiente alpino: esempi nella Valle del Foscagno e al Passo del Mortirolo (Alpi Centrali, Italia). Tettonica Recente e Instabilità di Versante nelle Alpi Centrali, edited by: Pasquarè, G, Vol Spec CARIPLO, Milano 103–149

Gischig V, Preisig G, Eberhardt E (2016) Numerical investigation of seismically induced rock mass fatigue as a mechanism contributing to the progressive failure of deep-seated landslides. Rock Mech Rock Eng 49:2457–2478

Gudmundsson GH (1994) An order-of-magnitude estimate of the current uplift-rates in Switzerland caused by the Würm Alpine deglaciation. Eclogae Geol Helv 87:545–557

Gutiérrez F, Masana E, González Á et al (2009) Late Quaternary paleoseismic evidence on the Munébrega half-graben fault (Iberian Range, Spain). Int J Earth Sci 98:1691–1703. https://doi.org/10.1007/s00531-008-0319-y

Gutiérrez-Santolalla F, Acosta E, Ríos S et al (2005) Geomorphology and geochronology of sackung features (uphill-facing scarps) in the Central Spanish Pyrenees. Geomorphology 69:298–314. https://doi.org/10.1016/j.geomorph.2005.01.012

Guzzetti F, Esposito E, Balducci V et al (2009) Central Italy seismic sequence-induced landsliding: 1997–1998 Umbria-Marche and 2008–2009 l'Aquila cases. In: The next generation of research on earthquake-induced landslides: an International conference in commemoration of 10th anniversary of the Chi-Chi earthquake, pp 52–60

Guzzetti F, Peruccacci S, Rossi M, Stark CP (2007) Rainfall thresholds for the initiation of landslides in central and southern Europe. Meteorol Atmos Phys 98:239–267

Haas JN, Richoz I, Tinner W, Wick L (1998) Synchronous Holocene climatic oscillations recorded on the Swiss Plateau and at timberline in the Alps. Holocene 8:301–309

Hetényi G, Epard J-L, Colavitti L et al (2018) Spatial relation of surface faults and crustal seismicity: a first comparison in the region of Switzerland. Acta Geod Geophys 53:439–461. https://doi.org/10.1007/s40328-018-0229-9

Ivy-Ochs S, Kerschner H, Reuther A et al (2006) The timing of glacier advances in the northern European Alps based on surface exposure dating with cosmogenic^ 1^ 0Be,^ 2^ 6Al,^ 3^ 6Cl, and^ 2^ 1Ne. Spec Pap Geol Soc Am Spec 415:43

Kahle HG, Geiger A, Buerki B, Gubler E, Marti U, Wirth B, Rothacher M, Gurtner W, Beutler G, Bauersima I, and Pfiffner OA (1997) Recent crustal movements, geoid and density distribution: Contribution from integrated satellite and terrestrial measurements: in Pfiffner, O.A., et al, eds., Results of NRP 20: Deep structure of the Swiss Alps : Basel, Boston, Berlin, Birkhaüser Verlag, pp. 251-259

Keefer DK (1984) Landslides caused by earthquakes | GSA Bulletin | GeoScienceWorld. https://pubs.geoscienceworld.org/gsa/gsabulletin/article-abstract/95/4/406/202914. Accessed 16 Jul 2019

Keefer DK (2000) Statistical analysis of an earthquake-induced landslide distribution – the 1989 Loma Prieta, California event. Eng Geol 58:231–249. https://doi.org/10.1016/S0013-7952(00)00037-5

Knight J, Harrison S (2009)Periglacial and Paraglacial Processes and EnvironmentsGeological Society of London Special Publications, p. 320

Kremer K, Gassner-Stamm G, Grolimund R et al (2020) A database of potential paleoseismic evidence in Switzerland. J Seismol 24:247–262. https://doi.org/10.1007/s10950-020-09908-5

Kremer K, Wirth SB, Reusch A et al (2017) Lake-sediment based paleoseismology: Limitations and perspectives from the Swiss Alps. Quatern Sci Rev 168:1–18. https://doi.org/10.1016/j.quascirev.2017.04.026

Locati M, Camassi R, Rovida A, Ercolani E, Bernardini F, Castelli V, Caracciolo CH, Tertulliani A, Rossi A, Azzaro R, D'Amico S, Antonucci A (2022) Database Macrosismico Italiano (DBMI15), versione 4.0. Istituto Nazionale di Geofisica e Vulcanologia (INGV). https://doi.org/10.13127/DBMI/DBMI15.4

Magny M, Combourieu-Nebout N, De Beaulieu J-L et al (2013) North–south palaeohydrological contrasts in the central Mediterranean during the Holocene: tentative synthesis and working hypotheses. Clim Past 9:2043–2071

Magny M, Galop D, Bellintani P et al (2009) Late-Holocene climatic variability south of the Alps as recorded by lake-level fluctuations at Lake Ledro, Trentino, Italy. Holocene 19:575–589

Magny M, Joannin S, Galop D et al (2012) Holocene palaeohydrological changes in the northern Mediterranean borderlands as reflected by the lake-level record of lake ledro, northeastern Italy. Quat Res 77:382–396. https://doi.org/10.1016/j.yqres.2012.01.005

Mariani GS, Zerboni A (2020) Surface geomorphological features of deep-seated gravitational slope deformations: a look to the role of lithostructure (N Apennines, Italy). Geosciences 10:334

Mayewski PA, Rohling EE, Stager JC et al (2004) Holocene climate variability. Quat Res 62:243–255

McCalpin JP (2009) A field techniques in paleoseismology–terrestrial environments. Int Geophys 95:29–118

McCalpin JP, Corominas J (2019) Postglacial deformation history of sackungen on the northern slope of Pic d'Encampadana. Geomorphology, Andorra. https://doi.org/10.1016/j.geomorph.2019.04.007

McGuire B, Maslin MA (2012) Climate forcing of geological hazards. John Wiley & Sons

Michetti A, Giardina F, Livio F et al (2012) Active compressional tectonics, quaternary capable faults, and the seismic landscape of the Po Plain (N Italy). Ann Geophys

Michetti AM, Esposito E, Guerrieri L et al (2007) Environmental seismic intensity scale-ESI 2007. Memorie Descrittive Della Carta Geologica D'italia 74:41

Mörner N-A (2004) Active faults and paleoseismicity in Fennoscandia, especially Sweden. Primary structures and secondary effects. Tectonophysics 380:139–157. https://doi.org/10.1016/j.tecto.2003.09.018

Norton KP, Hampel A (2010) Postglacial rebound promotes glacial re-advances–a case study from the European Alps. Terra Nova 22:297–302

Onida M (2001) Deformazioni gravitative profonde: stato delle conoscenze e progresso delle ricerche in Italia. Tettonica recente e instabilità di versante nelle Alpi centrali CNR, Istituto per la Dinamica dei Processi Ambientali, Milano, Italy 35–74

Oswald P, Strasser M, Hammerl C, Moernaut J (2021) Seismic control of large prehistoric rockslides in the Eastern Alps. Nat Commun 12:1059. https://doi.org/10.1038/s41467-021-21327-9

Papadopoulos GA, Plessa A (2000) Magnitude–distance relations for earthquake-induced landslides in Greece. Eng Geol 58:377–386. https://doi.org/10.1016/S0013-7952(00)00043-0

Pasquaré G (ed) (2001) Tettonica recente e instabilità di versante nelle Alpi Centrali. Fondazione CARIPLO per la Ricerca Scientifica; CNR-Istituto per la Dinamica dei Processi Ambientali – Milano

Pelfini M, Leonelli G, Trombino L et al (2014) New data on glacier fluctuations during the climatic transition at~ 4,000 cal. year BP from a buried log in the Forni Glacier forefield (Italian Alps). Rend Lincei 25:427–437

Peruccacci S, Brunetti MT, Luciani S et al (2012) Lithological and seasonal control on rainfall thresholds for the possible initiation of landslides in central Italy. Geomorphology 139:79–90

Poschinger AV, Wassmer P, Maisch M (2006) The Flims rockslide: history of interpretation and new insiights. In: Evans SG, Mugnozza GS, Strom A, Hermanns RL (eds) Landslides from Massive Rock Slope Failure. Springer, Netherlands, Dordrecht, pp 329–356

Prager C, Zangerl C, Patzelt G, Brandner R (2008) Age distribution of fossil landslides in the Tyrol (Austria) and its surrounding areas. Nat Hazard 8:377–407. https://doi.org/10.5194/nhess-8-377-2008

Prestininzi A, Romeo R (2000) Earthquake-induced ground failures in Italy. Eng Geol 58:387–397. https://doi.org/10.1016/S0013-7952(00)00044-2

Rapuc W, Arnaud F, Sabatier P et al (2022) Instant sedimentation in a deep Alpine lake (Iseo, Italy) controlled by climate, human and geodynamic forcing. Sedimentology sed.12972. https://doi.org/10.1111/sed.12972

Reimer PJ, Austin WEN, Bard E et al (2020) The IntCal20 northern hemisphere radiocarbon age calibration curve (0–55 cal kBP). Radiocarbon 62:725–757. https://doi.org/10.1017/RDC.2020.41

Rovida A, Locati M, Camassi R, Lolli B, Gasperini P, Antonucci A (2022) Catalogo Parametrico dei Terremoti Italiani (CPTI15), versione 4.0. Istituto Nazionale di Geofisica e Vulcanologia (INGV). https://doi.org/10.13127/CPTI/CPTI15.4

Sanchez G, Rolland Y, Corsini M et al (2010) Relationships between tectonics, slope instability and climate change: cosmic ray exposure dating of active faults, landslides and glacial surfaces in the SW Alps. Geomorphology 117:1–13. https://doi.org/10.1016/j.geomorph.2009.10.019

Schlüchter C, Bini A, Buoncristiani JF, Coutterand S, Ellwanger D, Felber M, et al (2009) Die Schweiz während des letzteiszeitlichen Maximums (LGM), 1: 500 000. GeoKarten500. Wabern: Bundesamt für Landestopografie swisstopo

Schmid SM, Aebli HR, Heller F, Zingg A (1989) The role of the Periadriatic Line in the tectonic evolution of the Alps. Geol Soc Spec Publ 45:153–171. https://doi.org/10.1144/GSL.SP.1989.045.01.08

Schnellmann M, Anselmetti FS, Giardini D et al (2002) Prehistoric earthquake history revealed by lacustrine slump deposits. Geology 30:1131–1134. https://doi.org/10.1130/0091-7613(2002)030%3c1131:PEHRBL%3e2.0.CO;2
Schumacher ME, Laubscher HP (1996) 3D crustal architecture of the Alps-Apennines join–a new view on seismic data. Tectonophysics 260:349–363
Schweingruber FH (1978) Microscopic Wood Anatomy, Mikroskopische Holzanatomie, Anatomie microscopique du bois. Swiss Federal Institute for Forest, Snow and Landscape Research (Eidgenössische Forschungsanstalt für Wald, Schnee und Landschaft), Birmensdorf (CH). 226 pp
Schweingruber FH (1990) Anatomy of European woods, Anatomie Europäischer Hölzer. Swiss Federal Institute for Forest, Snow and Landscape Research (Eidgenössische Forschungsanstalt für Wald, Schnee und Landschaft); Birmensdorf (CH). 800 pp
Segoni S, Piciullo L, Gariano SL (2018) A review of the recent literature on rainfall thresholds for landslide occurrence. Landslides 15:1483–1501
Sileo G, Giardina F, Livio F et al (2007) Remarks on the Quaternary tectonics of the Insubria Region (Lombardia, NW Italy, and Ticino, SE Switzerland). B Soc Geol Ital 126:411
Siletto GB, Spalla MI, Tunesi A et al (1990) Structural analysis in the Lario basement (Central Southern Alps, Italy). Memorie Della Soc Geol Ital 45:93–100
Soil Survey Staff (2014) Keys to Soil Taxonomy, 12th Edn Washington. DC: Natural Resources Conservation Service, United States Department of Agriculture [Google Scholar]
Spalla MI, Di Paola S, Gosso G et al (2002) Mapping tectono-metamorphic histories in the Lake Como basement (Southern Alps, Italy). Mem Di Sci Geol 54:101–134
Strasser M, Monecke K, Schnellmann M, Anselmetti FS (2013) Lake sediments as natural seismographs: a compiled record of Late Quaternary earthquakes in Central Switzerland and its implication for Alpine deformation. Sedimentology 60:319–341. https://doi.org/10.1111/sed.12003
Tibaldi A, Rovida A, Corazzato C (2004) A giant deep-seated slope deformation in the Italian Alps studied by paleoseismological and morphometric techniques. Geomorphology 58:27–47. https://doi.org/10.1016/S0169-555X(03)00184-3
Trauth MH, Alonso RA, Haselton KR et al (2000) Climate change and mass movements in the NW Argentine Andes. Earth Planet Sci Lett 179:243–256. https://doi.org/10.1016/S0012-821X(00)00127-8
Trauth MH, Bookhagen B, Marwan N, Strecker MR (2003) Multiple landslide clusters record Quaternary climate changes in the northwestern Argentine Andes. Palaeogeogr Palaeoclimatol Palaeoecol 194:109–121. https://doi.org/10.1016/S0031-0182(03)00273-6
Trigila A, Iadanza C (2008) Landslides in Italy. Special Report 83. ISPRA, Roma
Trigila A, Iadanza C, Spizzichino D (2010) Quality assessment of the Italian Landslide Inventory using GIS processing. Landslides 7:455–470
van Loon AJ, Pisarska-Jamroży M, Nartišs M et al (2016) Seismites resulting from high-frequency, high-magnitude earthquakes in Latvia caused by Late Glacial glacio-isostatic uplift. J Palaeogeogr 5:363–380. https://doi.org/10.1016/j.jop.2016.05.002
Viganò A, Rossato S, Martin S et al (2021) Large landslides in the Alpine valleys of the Giudicarie and Schio-Vicenza tectonic domains (NE Italy). J Maps 17:197–208. https://doi.org/10.1080/17445647.2021.1880979
Wang F, Fan X, Yunus AP et al (2019) Coseismic landslides triggered by the 2018 Hokkaido, Japan (M w 6.6), earthquake: spatial distribution, controlling factors, and possible failure mechanism. Landslides 16:1551–1566
Wirth SB, Glur L, Gilli A, Anselmetti FS (2013) Holocene flood frequency across the Central Alps – solar forcing and evidence for variations in North Atlantic atmospheric circulation. Quatern Sci Rev 80:112–128. https://doi.org/10.1016/j.quascirev.2013.09.002
WRB, I.W.g (2014) World Reference Base for Soil Resources 2014. International soil classification system for naming soils and creating legends for soil maps. in: FAO (Ed.).
Zanchetta G, Bar-Matthews M, Drysdale RN et al (2014) Coeval dry events in the central and eastern Mediterranean basin at 5.2 and 5.6 ka recorded in Corchia (Italy) and Soreq caves (Israel) speleothems. Glob Planet Chang 122:130–139
Zerathe S, Lebourg T, Braucher R, Bourlès D (2014) Mid-Holocene cluster of large-scale landslides revealed in the Southwestern Alps by 36Cl dating. Insight on an Alpine-scale landslide activity. Quatern Sci Rev 90:106–127. https://doi.org/10.1016/j.quascirev.2014.02.015
Zerboni A, Mariani GS, Castelletti L et al (2019) Was the Little Ice Age the coolest Holocene climatic period in the Italian central Alps?. Prog Phys Geogr Earth Environ 0309133319881105. https://doi.org/10.1177/0309133319881105
Zerboni A, Trombino L, Cremaschi M (2011) Micromorphological approach to polycyclic pedogenesis on the Messak Settafet plateau (central Sahara): Formative processes and palaeoenvironmental significance. Geomorphology 125:319–335
Zerboni A, Trombino L, Frigerio C et al (2015) The loess-paleosol sequence at Monte Netto: a record of climate change in the Upper Pleistocene of the central Po Plain, northern Italy. J Soils Sediments 15:1329–1350. https://doi.org/10.1007/s11368-014-0932-2

F. A. Livio (✉) · **M. F. Ferrario** · **E. Martinelli**
Dipartimento Di Scienza Ed Alta Tecnologia, Università Degli Studi Dell'Insubria, Como, CO, Italy
Email: franz.livio@uninsubria.it

A. Zerboni
Dipartimento Di Scienze Della Terra "A. Desio", Università Degli Studi Di Milano, Milan, Italy

G. S. Mariani
Dipartimento Di Scienze Chimiche E Geologiche, Università Degli Studi Di Cagliari, Cagliari, Italy

R. Amit
Geological Survey of Israel, Jerusalem, Israel